

Non-ideal atom-light interfaces: modeling real-world effects

M. Koschorreck* and M. W. Mitchell

ICFO - Institut de Ciències Fotoniques, Mediterranean Technology Park, 08860 Castelldefels (Barcelona), Spain

We present a model which describes coherent and incoherent processes in continuous-variable atom-light interfaces. We assume Gaussian states for light and atoms and formulate the system dynamics in terms of first and second moments of the angular momentum operators. Spatial and temporal inhomogeneities in light and atom variables are incorporated by partitioning the system into small homogeneous segments. Furthermore, other experimental imperfections as for instance limited detector time-resolution and atomic motion are simulated. The model is capable of describing many experimental situations ranging from room temperature vapor cells to sub-mK atomic clouds. To illustrate the method, we calculate the effect of detector time-resolution, spatial inhomogeneities and atomic motion on the spin squeezing dynamics of rubidium 87 on the D_2 transition.

PACS numbers: 03.65.Ud, 42.50.Dv, 05.30.Ch, 03.65.Ta, 32.80.-t

I. INTRODUCTION

In the last decade, many pioneering experiments have demonstrated quantum information processing with continuous variables in atomic and photonic systems. Atomic spin squeezing can overcome the standard quantum limit in magnetometry [1]. Macroscopic numbers of atoms can serve as a memory of a quantum state of light [2]. A variety of atomic systems have been proposed or demonstrated, including hot atoms in cells and cold atoms in magneto-optical traps and in optical dipole traps. The conditions vary greatly from system to system, notably in number of atoms, from $\sim 10^{12}$ in cells to $\sim 10^6$ in dipole traps, in temperature, from ~ 300 K in cells to ~ 30 μ K in atom traps, and in the time-scale of the interactions, from milliseconds in cells to microseconds in cold atoms. At the same time, a variety of other physical effects, such as loss and decoherence of atoms, scattering and diffraction of light, and inhomogeneous coupling of the light and atomic variables are present to varying degrees in these systems.

We demonstrate here that these many effects can be treated within a single framework. We work with Gaussian states, where coherent interactions and incoherent loss and decoherence processes have been studied. Previous work on inhomogeneity has included mode matching [3] and introduction of weighted variables [4]. In some cases decoherence effects due to inhomogeneous coupling have been identified [5]. Here we show how the model of Madsen *et al.* [6], when applied to the physical angular momentum and Stokes operators, can be naturally extended to include inhomogeneities as well as transport processes such as movement of atoms.

In the first part we review some important definitions of angular momentum operators for atoms and light. We introduce the method of segmentation and give its mathematical description in compact form. We give a general

description of physical processes including coherent light-atom interaction, coherent and incoherent transport processes, and projective measurements. Incoherent transport is used to describe loss and decoherence.

In the second part we apply these techniques to calculate the effect on spin squeezing of: imperfect detector temporal resolution, spatial inhomogeneities in atoms and light, and atomic motion.

II. PHYSICAL SYSTEM AND MATHEMATICAL MODEL

A. Continuous variables for light and atoms

Polarized light in the framework of continuous variables can be described in terms of the Stokes operators

$$\hat{S}_x = \frac{\hbar}{2} \mathbf{a}^\dagger \boldsymbol{\sigma}_x \mathbf{a} \quad \hat{S}_y = \frac{\hbar}{2} \mathbf{a}^\dagger \boldsymbol{\sigma}_y \mathbf{a} \quad \hat{S}_z = \frac{\hbar}{2} \mathbf{a}^\dagger \boldsymbol{\sigma}_z \mathbf{a} . \quad (1)$$

Here $\mathbf{a} \equiv [\hat{a}_+, \hat{a}_-]^T$ and \hat{a}_+, \hat{a}_- are annihilation operators for circular plus and minus polarization, respectively and $\boldsymbol{\sigma}_x, \boldsymbol{\sigma}_y$, and $\boldsymbol{\sigma}_z$ are the Pauli matrices. The Stokes operators have the same commutation relations as angular momentum operators. In many situations of interest, one polarization component is strong. Here we consider linearly polarized light:

$$\langle \hat{S}_x \rangle = \frac{1}{2} \hbar N_L \equiv S_x \quad \text{and} \quad \langle \hat{S}_y \rangle, \langle \hat{S}_z \rangle = 0$$

where N_L is the number of photons. A coherent polarization state can be expressed as an angular momentum - [7] or spin and atomic - [8, 9] coherent state. All of them have in common that the variances orthogonal to the main “spin” are

$$\text{var}(\hat{S}_y) = \text{var}(\hat{S}_z) = \frac{1}{4} \hbar^2 N_L .$$

Along this direction we have either $\text{var}(\hat{S}_x) = \hbar^2 N_L / 4$ [7] or $\text{var}(\hat{S}_x) = 0$ [8, 9]. For $N_L \gg 1$, we can substitute the

*Electronic address: marco.koschorreck@icfo.es; URL: www.icfo.es

operator \hat{S}_x by its expectation value. Hence, quantum polarization features are then solely contained in \hat{S}_y and \hat{S}_z . Geometrically, we are approximating a portion of the Poincaré sphere as a plane, the geometry of the harmonic-oscillator phase space. Formally, this is referred to as the contraction from $SU(2)$ to the Heisenberg-Weyl group [8]. Consequently, the commutator for \hat{S}_y and \hat{S}_z is not operator valued, as it would be in the $SU(2)$ algebra. Instead of writing $[\hat{S}_i, \hat{S}_j] = i\hbar\epsilon_{ijk}\hat{S}_k$, we have $[\hat{S}_y, \hat{S}_z] = i\hbar S_x$ and $[\hat{S}_x, \hat{S}_{y/z}] = 0$. Apart from normalization, these are the commutation relations for the generators of the Lie algebra in the Heisenberg-Weyl group.

For atoms, we similarly describe the collective spin of a collection of atoms with the angular momentum operators

$$\hat{J}_x = \frac{\hbar}{2} \mathbf{b}^\dagger \boldsymbol{\sigma}_x \mathbf{b} \quad \hat{J}_y = \frac{\hbar}{2} \mathbf{b}^\dagger \boldsymbol{\sigma}_y \mathbf{b} \quad \hat{J}_z = \frac{\hbar}{2} \mathbf{b}^\dagger \boldsymbol{\sigma}_z \mathbf{b} . \quad (2)$$

defined in terms of bosonic operators $\mathbf{b} \equiv [\hat{b}_\uparrow, \hat{b}_\downarrow]^T$. The states $|\uparrow\rangle, |\downarrow\rangle$ are two degenerate atomic ground states. These could be the states of a spin-1/2 atom, as in the proposal of Kuzmich *et al.* [10], or more practically, two ground states of an alkali atom. Later, we will consider the case of $F=1$, where $|\uparrow\rangle \equiv |F=1, m_F=-1\rangle$, $|\downarrow\rangle \equiv |F=1, m_F=+1\rangle$ [11]. The operator $\hat{\mathbf{J}}$ then describes a pseudo-spin, with angular momentum commutation relations but without spin-like behavior under spatial rotations.

We assume the atoms are polarized along a certain direction, so that one angular momentum component can be treated classically and the two orthogonal components carry the quantum properties. For x polarization,

$$\langle \hat{J}_x \rangle = \frac{1}{2} \hbar N_A \equiv J_x \quad \text{and} \quad \langle \hat{J}_y \rangle, \langle \hat{J}_z \rangle = 0 ,$$

and the variances are

$$\text{var}(\hat{J}_y) = \text{var}(\hat{J}_z) = \frac{1}{4} \hbar^2 N_A .$$

B. Partitioning and covariance matrix

A central goal of this work is to include spatial inhomogeneities in a description of the light-atom interaction. In cell experiments, the atomic ensemble has a constant number density while a cold trapped sample can be highly inhomogeneous. In almost all experiments, the light distribution is inhomogeneous, e.g. from a Gaussian beam.

We split the inhomogeneous ensembles of atoms and light into several *segments*. That is, we define angular momentum variables for the atom segments $\hat{\mathbf{J}}^{(k,l)}$, and for the light segments $\hat{\mathbf{S}}^{(k,l')}$, with $[\hat{J}_\lambda^{(k,l)}, \hat{J}_\mu^{(m,n)}] = i\hbar\epsilon_{\lambda\mu\nu}\hat{J}_\nu^{(k,l)}\delta_{km}\delta_{ln}$ and $[\hat{S}_\lambda^{(k,l)}, \hat{S}_\mu^{(m,n)}] = i\hbar\epsilon_{\lambda\mu\nu}\hat{S}_\nu^{(k,l)}\delta_{km}\delta_{ln}$. The segments orthogonal to the direction of light propagation are called *transverse seg-*

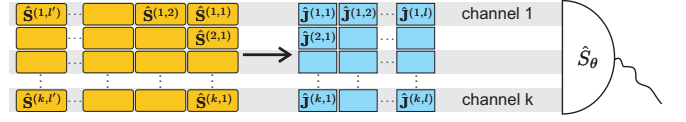


Figure 1: Schematic of partitioned atom-light interface. See text for details.

ments (first index) and along the direction of light propagation, *longitudinal segments* (second index) (cf. Fig. 1). Here we do the segmentation in two dimensions only; the extension to the third is straightforward. In order to stay within the assumptions of the group contraction, we have to ensure that the particle number in each segment is itself large, i.e., $N_A^{(k,l)} \gg 1$ and $N_L^{(k,l')} \gg 1$. The total angular momenta for atoms and light are

$$\hat{\mathbf{J}} = \sum_{k,l} \hat{\mathbf{J}}^{(k,l)} \quad \text{and} \quad \hat{\mathbf{S}} = \sum_{k,l'} \hat{\mathbf{S}}^{(k,l')} . \quad (3)$$

We define a *channel* as the set of segments (light and atoms) which have the same transverse index k .

We assume that the ensembles both of atoms and photons can be described as Gaussian states in the harmonic oscillator phase space and that all operations we apply will map them into Gaussian states. For a single segment of light we can use equation (1) and define a phase space vector as

$$\hat{\mathbf{s}}^{(k,l)} \equiv \begin{bmatrix} \hat{S}_y^{(k,l)} \\ \hat{S}_z^{(k,l)} \end{bmatrix} = \frac{\hbar}{2} \left(\mathbf{a}^{(k,l)} \right)^\dagger \begin{Bmatrix} \sigma_y \\ \sigma_z \end{Bmatrix} \mathbf{a}^{(k,l)} , \quad (4)$$

and similarly for atoms

$$\hat{\mathbf{j}}^{(k,l)} \equiv \begin{bmatrix} \hat{J}_y^{(k,l)} \\ \hat{J}_z^{(k,l)} \end{bmatrix} = \frac{\hbar}{2} \left(\mathbf{b}^{(k,l)} \right)^\dagger \begin{Bmatrix} \sigma_y \\ \sigma_z \end{Bmatrix} \mathbf{b}^{(k,l)} . \quad (5)$$

In a common phase space for atoms and light we define an overall phase space vector in terms of angular momentum operators as

$$\hat{\mathbf{v}} = \left[\hat{\mathbf{j}}^{(1,1)}, \dots, \hat{\mathbf{j}}^{(k,l)}, \hat{\mathbf{s}}^{(1,1)}, \dots, \hat{\mathbf{s}}^{(k,l')} \right]^T \quad (6)$$

which is readily rewritten as the direct sum of phase space vectors of the sub-systems for atoms (A) and light (L)

$$\hat{\mathbf{v}} = \hat{\mathbf{v}}_A \oplus \hat{\mathbf{v}}_L \quad (7)$$

Gaussian states are completely characterized by their first and second moments. First moments $\langle \hat{\mathbf{v}} \rangle$ represent a displacement in phase space. Second moments or variances are given by

$$\boldsymbol{\gamma} = \frac{1}{2} \left\langle \hat{\mathbf{v}} \wedge \hat{\mathbf{v}} + (\hat{\mathbf{v}} \wedge \hat{\mathbf{v}})^T \right\rangle - \langle \hat{\mathbf{v}} \rangle \wedge \langle \hat{\mathbf{v}} \rangle \quad (8)$$

which is the covariance matrix. For our purpose of examining entanglement and squeezing properties, only the

second moments are of interest. We can write the covariance matrix of the joint atom-light system as

$$\gamma = \begin{bmatrix} \mathbf{A} & \mathbf{C} \\ \mathbf{C}^T & \mathbf{L} \end{bmatrix} \quad (9)$$

where \mathbf{C} describes correlation between atoms (\mathbf{A}) and light (\mathbf{L}).

III. UNIFIED DESCRIPTION OF PHYSICAL PROCESSES

The dynamics of $\hat{\mathbf{v}}$ and γ is calculated by difference equations which describe small but finite changes between time-steps. This allows us to model coherent light-atom interactions, losses and decoherence, measurement and transport processes in a consistent way.

The phase space vector and covariance matrix are updated in finite time steps τ as

$$\hat{\mathbf{v}}(t + \tau) = \mathbf{F}_\tau(\hat{\mathbf{v}}(t)) . \quad (10)$$

The time step is chosen to be the duration of a longitudinal light segment. It should be short enough that a longitudinal segment can be considered homogeneous, but still contain many photons.

We note that in most experiments the atomic sample is much shorter than the coherence time of the light pulse, which means that in each channel only one longitudinal light segment will overlap with the ensemble at most times. In addition, the effect of the several longitudinal atomic segments is, from the light's perspective, sequential: $\hat{\mathbf{s}}^{(n,1)}$ interacts with $\hat{\mathbf{j}}^{(n,1)}$ then with $\hat{\mathbf{j}}^{(n,2)}$, and so forth. In the time $t = (m-1)\tau$ to $t < m\tau$, the $\hat{\mathbf{s}}^{(n,m)}$ interacts with all atomic segments $\hat{\mathbf{j}}^{(n,l)}$ in the n -th channel.

A. Coherent effects

For effects described by a Hamiltonian \hat{H} which is linear in the elements of the phase-space vector $\hat{\mathbf{v}}$, the phase space vector evolves as (to lowest order in τ),

$$\hat{\mathbf{v}}(t + \tau) = \hat{\mathbf{v}}(t) - \frac{i\tau}{\hbar} [\hat{\mathbf{v}}, \hat{H}] \equiv \mathbf{T}_\tau \hat{\mathbf{v}}(t) . \quad (11)$$

The last equality, which expresses the change in $\hat{\mathbf{v}}$ in terms of a matrix \mathbf{T}_τ , is possible by the linearity of the Hamiltonian and the c-number-valued commutation relations. The covariance matrix evolves as

$$\gamma(t + \tau) = \mathbf{T}_\tau \gamma(t) \mathbf{T}_\tau^T . \quad (12)$$

1. Single species effects

A magnetic field acts solely on the atomic spin and leaves the light unchanged. Owing to the pseudo-spin

character of $\hat{\mathbf{J}}$ we take only magnetic fields along the z axis into account. Such a field results in a rotation about the z axis in the Bloch sphere. To ensure the validity of the group contraction we also limit the rotations to small angles. The Hamiltonian for the segment (k, l) is

$$\hat{H}_{\text{magn}}^{(k,l)} = \mu_B g_F \hat{J}_z^{(k,l)} B_z^{(k,l)} . \quad (13)$$

Where, μ_B is the Bohr magneton and g_F the Landé factor. This description includes homogeneous as well as inhomogeneous magnetic fields.

2. Atom-Light Interaction

For a homogeneous system of light and atoms off-resonant interaction gives rise to an effective Hamiltonian. For the $F = 1$ pseudo-spin system, it has the form

$$\hat{H}_{\text{eff}} \propto (\alpha^{(0)} + \frac{\alpha^{(2)}}{3}) \hat{S}_0 \hat{J}_0 + \alpha^{(1)} \hat{S}_z \hat{J}_z + \alpha^{(2)} (\hat{S}_x \hat{J}_x + \hat{S}_y \hat{J}_y) \quad (14)$$

where $\alpha^{(0)}$, $\alpha^{(1)}$, and $\alpha^{(2)}$ are the scalar, vector and tensor components of the polarizability [12].

For brevity, we will write this interaction as $\hat{H}_{\text{eff}}(\hat{\mathbf{S}}, \hat{\mathbf{J}})$. As the light pulse propagates through the medium, the effects of $\hat{H}_{\text{eff}}(\hat{\mathbf{s}}^{(n,1)}, \hat{\mathbf{j}}^{(n,1)})$, $\hat{H}_{\text{eff}}(\hat{\mathbf{s}}^{(n,1)}, \hat{\mathbf{j}}^{(n,2)})$, and so forth are applied in sequence to the covariance matrix. Note that loss and decoherence may be applied between these coherent evolutions.

B. Noise considerations

In addition to Hamiltonian evolution, loss, transport, and decoherence of atoms and/or photons can be described. These processes introduce extra noise into the system. A fully general description of a noisy Gaussian process is the Gaussian completely-positive map (GP), which acts on the covariance matrix as

$$\gamma' = \mathbf{M} \gamma \mathbf{M}^T + \mathbf{N} \quad (15)$$

where the real matrix \mathbf{M} transforms the phase space vector and the real symmetric matrix \mathbf{N} describes added noise. These must obey [13]

$$\mathbf{N} + i\mathbf{\Sigma}' - i\mathbf{M}\mathbf{\Sigma}\mathbf{M}^T \geq 0 \quad (16)$$

where $i\Sigma_{ij} \equiv [v_i, v_j]$ and $\mathbf{\Sigma}'$, similarly defined, are commutation matrices before and after the transformation (note that the commutation relations, which include the "classical" components J_x, S_x can change due to loss and decoherence). This places a lower limit on the noise introduced. Specifically,

$$\mathbf{N} = |\mathbf{i}\mathbf{\Sigma}' - i\mathbf{M}\mathbf{\Sigma}\mathbf{M}^T| , \quad (17)$$

where $|\cdot|$ indicates the matrix absolute value, is the minimal symmetric matrix to satisfy (16).

1. Loss and Decoherence from photon scattering

Inevitably, the coherent interaction of equation (14) will be accompanied by spontaneous emission of photons, producing also incoherent changes in the atomic state. We use equation (15) to calculate the effect of loss and decoherence of atoms and photons. Here "loss" of atoms refers to the decay of atoms into meta-stable states which do not interact with the light. Decay of atoms into the $|\uparrow\rangle, |\downarrow\rangle$ states can cause decoherence of the spin state. While loss is not present in the ideal spin-1/2 system proposed by Kuzmich *et al.* [10], in alkali metal atoms both processes are observed. For light there is no decoherence process since spontaneously emitted photons scatter into all possible spatial modes and are counted as losses.

The covariance matrix transforms as

$$\gamma(t + \tau) = \mathbf{M}_\tau \gamma(t) \mathbf{M}_\tau^T + \mathbf{N}_\tau, \quad (18)$$

where the decay is described by

$$\mathbf{M}_\tau = (1 - \eta_\tau) \mathbb{I}_2 \oplus (1 - \varepsilon) \mathbb{I}_2. \quad (19)$$

Here η_τ and ε are scattering probabilities for an atom and a photon, respectively. For rubidium 87 these are given in terms of experimental parameters in the appendix. Noise will have the form $\mathbf{N}_\tau = \mathbf{N}_{\tau, \text{loss}} + \mathbf{N}_{\tau, \text{dec}}$ with (17) we get

$$\mathbf{N}_{\tau, \text{loss}} = \eta_\tau (1 - \eta_\tau) \frac{\hbar^2}{4} N_A \mathbb{I}_2 \oplus \varepsilon (1 - \varepsilon) \frac{\hbar^2}{4} N_L \mathbb{I}_2 \quad (20)$$

and

$$\mathbf{N}_{\tau, \text{dec}} = \rho \eta_\tau \frac{\hbar^2}{4} N_A \mathbb{I}_2 \oplus \mathbb{O}_2. \quad (21)$$

Here ρ is the fraction of the scattered atoms which return to the system, assumed to be in a mixed state. This model has been used in the literature [14] and serves to illustrate the method. A different model would be necessary to describe some processes, e.g., optical pumping. \mathbb{I}_2 is the identity matrix in two dimensions. \mathbb{O}_2 is the zero matrix and reflects the fact that we don't consider any decoherence for the light. For all simulations that follow in section IV we assume we have exclusively atomic decoherence and no loss, i.e., $\rho = 1$.

C. Projective Measurement

The next class of operations we can apply are measurements of atomic or light variables. While a measurement will collapse the value of an observable in a way that is fundamentally random, the resulting variances change in a way that is completely predictable: The variance of the measured observable becomes zero, the variance of the conjugate observable becomes large or infinite. The variances of other observables may also be reduced if they are correlated with the measured observable.

A measurement can be described by a projection matrix \mathcal{P} . For example, to measure a polarization component of the (n, i) light segment, $\hat{S}_\theta^{(n, i)} \equiv \cos \theta \hat{S}_y^{(n, i)} + \sin \theta \hat{S}_z^{(n, i)} \equiv (\mathbf{p}_\theta^{(n, i)})^T \cdot \mathbf{v}$, the projector would be the outer product $\mathcal{P} = \mathbf{p}_\theta^{(n, i)} \wedge \mathbf{p}_\theta^{(n, i)}$. In practical situations, measurement of a light variable also implies that a light segment has reached a detector and thus is removed from the problem, reducing the dimension of the vector \mathbf{v} . Upon measurement, the covariance matrix becomes

$$\gamma' = |\gamma - \gamma(\mathcal{P}\gamma\mathcal{P})^{-}\gamma^T|_{(n, i)}. \quad (22)$$

Where $|\dots|_{(n, i)}$ removes the column and row corresponding to the measured, and no longer existing, light segment (n, i) . $(\dots)^{-}$ indicates the Moore-Penrose pseudoinverse. Equation (22) is well known in mathematical statistics to compute the conditional covariance matrix of multivariate normal distributions [15]. A more detailed introduction of Gaussian operations on Gaussian states can be found in [16, 17].

For the calculations in Part 2, we consider a large-area detector, i.e., one which does not distinguish between different channels (see Fig. 1). Therefore, we define the measured light variable to be

$$\hat{S}_\theta^{(l)} = \sum_{k=1} \hat{S}_\theta^{(k, l)}. \quad (23)$$

D. Combining effects

When several effects are present at the same time-step, they are applied sequentially. The order of application can influence the results of the calculation if the time-step is not small. For example, when the light-atom interaction of Eq. (12) and noise of Eq. (18) are both considered, we can have

$$\gamma(t + \tau) = \mathbf{M}_\tau \mathbf{T}_\tau \gamma(t) \mathbf{T}_\tau^T \mathbf{M}_\tau + \mathbf{N}_\tau \quad (24)$$

or

$$\gamma(t + \tau) = \mathbf{T}_\tau [\mathbf{M}_\tau \gamma(t) \mathbf{M}_\tau + \mathbf{N}_\tau] \mathbf{T}_\tau^T, \quad (25)$$

depending on which effect is applied first. Physically, this ordering has no meaning, and in the limit of small time steps τ , both (24) and (25) give the same result. In the simulations that follow, we reduce τ until the effect of the ordering is negligible.

IV. RESULTS

Now we give three examples how the model can be applied in the context of atomic spin squeezing. For all simulations we consider a cold ensemble of rubidium 87 atoms in a dipole trap. The set of used parameters can be found in the appendix. It is well known that for large

detunings from resonance we can reduce the dipole interaction Hamiltonian (14) to

$$\hat{H}_{\text{eff}} \left(\hat{\mathbf{s}}^{(k,j)}, \hat{\mathbf{j}}^{(k,l)} \right) = \frac{\hbar g^{(k,l)}}{\tau} \hat{S}_z^{(k,j)} \hat{J}_z^{(k,l)}. \quad (26)$$

The coupling constant $g^{(k,l)}$ is proportional to the vector polarizability $\alpha^{(1)}$ and defined in the appendix. Note, the Hamiltonian does not explicitly depend on τ because the Stokes operators are proportional to the flux of photons times τ . As initial states we assume a pulse of horizontally polarized light, i.e., $S_x = N_L \hbar/2$ and a coherent superposition of the Zeeman substates $|F=1, m_F=-1\rangle$ and $|F=1, m_F=1\rangle$, i.e., $J_x = N_A \hbar/2$.

The effect of the Hamiltonian (26) on the light is a rotation of \hat{S}_x about the z -axis by an amount proportional to \hat{J}_z . At the same time, \hat{J}_z is not altered in this process. A projective measurement of \hat{S}_y provides information about, and thus reduces the uncertainty of, \hat{J}_z . If both input states are minimum uncertainty states, spin squeezing is obtained. To monitor the evolution of this process we evaluate $2\text{Var}(\hat{J}_z)/J_x$ which is also known as the spin squeezing parameter [18]. For squeezed states it will become less than unity. The smaller the spin squeezing parameter the higher the degree of spin squeezing. There are other criteria, for instance by Wineland *et al.* [1] derived in the context of precision spectroscopy. Regardless which of the definitions is applied, we obtain the same qualitative results.

To make the comparison between different experimental situations clearer, we normalize the timescale. We can define a time when the rotation of the light polarization due to the atom-light interaction (26) exceeds the shot noise of the photons, i.e., when the signal-to-noise ratio becomes one. We want this time to be characteristic for the system as a whole. Therefore, we neither partition atoms nor light and get

$$t_0 = \frac{4}{\hbar^4 G^2 N_A \Phi}. \quad (27)$$

Where G is the collective interaction strength, N_A the number of atoms and Φ the photon-flux. A detailed derivation is given in the appendix.

A. Detector time-resolution

As a first example, we study the influence of the detector time-resolution on the amount of spin squeezing and show the importance of correct modeling of pulsed experiments even for pulses much shorter than the detector time resolution.

We define an *ideal detector* as one capable of detecting individual light segments. The covariance matrix would be updated in accordance to (22) each time a light segment hits the detector. In contrast, we say a detector has no time-resolution if it detects all segments at the same

time. Mathematically, the measured variable is the sum of all n light segments

$$\hat{S}_y^{(1)} = \sum_{l=1}^n \hat{S}_y^{(1,l)}, \quad (28)$$

and we apply the transformation (22) to the whole covariance matrix. (For simplicity we assume only one atomic segment. Nonetheless, we keep the transverse index to avoid confusion.) The projector has the form

$$\mathcal{P} = \mathbb{O}_2 \oplus \frac{1}{n} \mathbb{U}_n \otimes \mathbb{I}_2. \quad (29)$$

Where \mathbb{U}_n is the unit matrix of rank n .

In Fig. 2 we show the results for both having (a) perfect and (b) no temporal resolution. In the case of no temporal resolution, the achievable spin squeezing is reduced at longer timescales. This is understood if we compare the information carried by different longitudinal light segments. Early light segments interact with the initial atomic state and later ones with a noisier version of it. If the detector is lacking temporal resolution all this different information is mixed.

Now we compare the results to calculations which neglect all dynamics during the pulse duration, e.g., in [4]. We call this type of model “zero-dimensional” because it treats the light-atom interaction as a point-like event in time. Therefore, we assume that the light pulse is not partitioned into longitudinal segments. Curve (c) and (d) in Fig. 2 show the results if the noise is added after (cf. Eq. 24) and before (cf. Eq. 25) the interaction, respectively. It becomes obvious that even in the case of a pulsed experiment it is important to model light as a stream of sufficiently short segments.

B. Spatial inhomogeneities

In many experiments inhomogeneities in light or atomic distributions are present. We give two examples for typical situations that can arise. As the simplest test model we assume an atomic ensemble which consists of two equally sized transverse segments.

For all the following calculations we assume an ideal detector. Furthermore, the total number of atoms N_A , the photon flux Φ , the total interaction cross section A , and all other parameters are fixed and stated in the appendix. The figure of merit is the variance of \hat{J}_z for the complete atomic ensemble

$$\text{var}(\hat{J}_z) = \text{var} \left(\sum_i \hat{J}_z^{(i)} \right). \quad (30)$$

To verify the validity of the segmentation model, we consider first a homogeneous atom distribution either as a single or as two segments. In both cases we observe the same results in the presence of atom-light interaction, loss and decoherence and transport processes, independent on

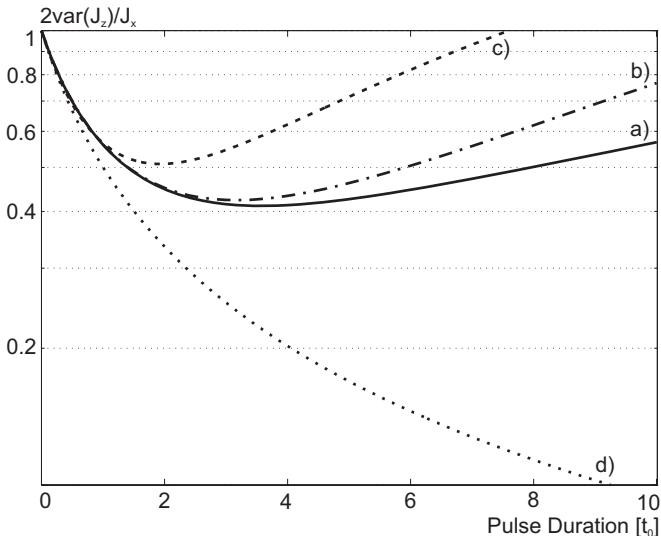


Figure 2: The spin squeezing achieved by using an ideal detector (a) and a detector with no temporal resolution (b) are shown. The parameters are given in appendix A. Two zero-dimensional calculations are given for comparison. In curve (c) the noise due to decoherence and loss was added after and in (d) before the interaction.

the segmentation. They reproduce the solid line (a) in Fig. 2).

The first example reflects the situation we would find for inhomogeneous light fields interacting with homogeneously distributed atoms. We model this with two channels of equal interaction cross-section $A/2$. We assume light is only present in one of the channels. The result is plotted as the dotted curve in Fig. 3. The overall spin squeezing is reduced. To explain this, we can evaluate both channels independently. One channel contains all the photons and the maximal obtainable amount of squeezing will be the same as for the homogeneous distribution (solid line in Fig. 2). This reflects a very important property in atomic spin squeezing. The achievable amount of squeezing does not depend on the intensity of light (supposed it is not zero) but rather on the optical depth of the atomic ensemble. For the second channel, without light, we expect no change in the atomic state. If we combine these two results, we get exactly the dotted curve shown in Fig. 3.

The second example is the inverse situation. The light beam has a larger cross-section than the atomic ensemble. We model this case by assuming all N_A atoms only in one of the channels and light homogeneously distributed over both. The result, plotted as the solid line in Fig. 3, seems surprising. We see the exact same dynamics as for the homogeneous case. In this situation two effects are compensating each other. The optical depth for the atoms is twice as large as in the previous examples and leads to larger spin squeezing. On the other hand, the light which does not interact with the atoms is also detected, and contributes noise but no additional infor-

mation about the atoms.

The two examples give some intuition about the influence of inhomogeneities. It is now straightforward to apply it to more interesting and complicated experimental cases.

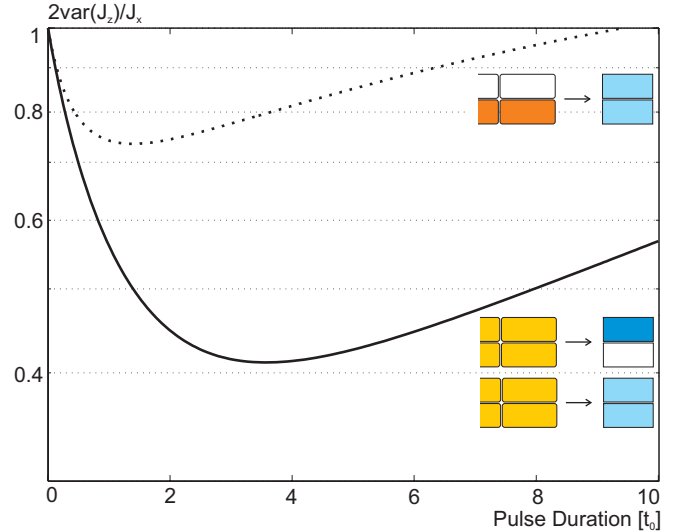


Figure 3: Two exemplary cases are compared to the homogeneous situation where light and atoms are evenly distributed over space. For more information see text.

C. Atomic motion

As a last application, we ask what happens when atoms can change places and go from one segment to another. This is a relevant question comparing different experimental situations. Atoms in vapor cells, for instance, have approximately room temperature. This corresponds to a root-mean-square (rms) velocity of hundreds of meters per second as opposed to a few tens of millimeters per second for dipole-trapped atoms. Typical timescales, t_0 , for the light-atom interaction are milliseconds and microseconds, respectively. Hence, atoms in vapor cells have moved around half a meter (effectively) whereas the atoms in the trap moved less than hundred nanometers. This suggests that for trapped atoms, any inhomogeneity in the light beam will be mapped onto them [23]. To find a more quantitative description, we introduce a mixing probability m_τ per time step τ and per atom. It is defined as the probability an atom would escape from one segment to another in one time step.

As in the previous section, we use the simple test model of two channels, where all the light is concentrated in one part and the atoms are homogeneously distributed over both. The real symmetric matrix describing the mixing is

$$\mathbf{M} = \begin{bmatrix} 1 - m_\tau & m_\tau \\ m_\tau & 1 - m_\tau \end{bmatrix} \otimes \mathbb{I}_2, \quad (31)$$

and the introduced noise is given by

$$\mathbf{N} = m_\tau (1 - m_\tau) \frac{\hbar^2}{4} N_A \begin{bmatrix} 1 & -1 \\ -1 & 1 \end{bmatrix} \otimes \mathbb{I}_2. \quad (32)$$

The noise matrix \mathbf{N} reflects two things. First, the individual variance in a single segment will increase. This is not surprising, because already correlated atoms leave the segment and uncorrelated atoms enter. Second, the variances of the total spin components are not altered by mixing. This is expected, since the choice of the partitioning is arbitrary and can have therefore no influence. An alternate way to derive \mathbf{N} and \mathbf{M} is sketched in [24]

As a concrete example we assume we have an ideal gas of atoms and derive the mixing probability from kinetic gas theory. The number of collisions per area and time in an ideal gas is known to be $R = N v_{\text{rms}} / (V \sqrt{6\pi})$. Where, N is the number of atoms in volume V , and their rms velocity is v_{rms} . From this we can calculate the rate at which individual atoms cross a surface of area A' , $r = RA'/N$. Furthermore, we assume that the atoms occupy a box of volume $V = A' \sqrt{A}$, where A is the interaction cross section of a segment. The rate can therefore be written as

$$r = \frac{v_{\text{rms}}}{\sqrt{6\pi A}}. \quad (33)$$

In the limit of small τ we can define a mixing probability as $m_\tau = r\tau$.

$$m_\tau = \frac{v_{\text{rms}}}{\sqrt{6\pi A}} \tau. \quad (34)$$

Where $v_{\text{rms}} = \sqrt{3k_B T/m}$ is the rms velocity of the atoms. This model is not an exact treatment of the different physical situations we find in vapor cells and atomic traps. Nevertheless, it suggests how atomic motion influences the formation of spin squeezing.

In Fig. 4 we plot the squeezing factor for different mixing probabilities. For $m_\tau/\tau \rightarrow 0$ (blue curves) we have the same situation as in the dotted curve of Fig. 3. For increasing mixing probability (red curves) we see that the squeezing is improved and the full amount (compared to the homogeneous situation, i.e., solid curve of Fig. 2) is achieved again. In this limit, when the inverse mixing rate becomes the same order of magnitude as t_0 , sufficient atomic movement is present that all the atoms get enough interaction to be uniformly squeezed. This suggests that approaches of matched variables, e.g., by Kuzmich *et al.* [4] are more relevant for cold atoms than for hot vapor cell experiments.

If we instead focus our attention only on the segment of atoms which is illuminated we see in plot b) of Fig. 4 that the spin squeezing for this segment reduces when the mixing probability increases. One can interpret this as a decoherence mechanism for the smaller segment [19].

V. CONCLUSION

We have presented a model to compute the dynamics of interacting light and atomic ensembles with Gaussian states. The model is based on covariance matrices for the quantum components of collective angular momentum operators and employs segmentation of the light and atom systems. The model is similar to that of Madsen *et al.* [6], but extends the segmentation to light and to the transverse directions. Also, we use angular momentum operators, rather than derived canonical operators, which give intuitive results and simplify partitioning. We show how to include many effects which arise in real experimental situations, including spatial and temporal inhomogeneities, atom motion, loss, and noise introduced by photon scattering.

Employing this model, we have made the following observations: The dynamics of spin squeezing requires time-dependent modeling, even when the atoms interact with optical pulses which are shorter than the detection system can resolve. At the same time, the detector time resolution has only a minor effect on the degree of spin squeezing under realistic conditions. The effect of spatial inhomogeneities in light and atoms have non-equivalent effects on spin squeezing: Concentration of the light into a sub-region of the atoms produces equal squeezing of the sub-region, but less squeezing of the entire ensemble, while concentration of the atoms into one sub-region of the light gives equal squeezing of the spin ensemble. Finally, we observe that atomic motion between an illuminated region and a non-illuminated one tends to degrade squeezing of the illuminated region while increasing squeezing of the entire atomic ensemble. This suggests that high-fidelity experiments should use probe pulses which are either much shorter, or much longer, than the time-scale of the atomic motion.

The model can straight-forwardly be adapted to more complicated experimental situations, for example a cold thermal cloud in a focused laser beam. Also, application to multi-pass schemes as proposed by Takeuchi *et al.* [20] or Sherson *et al.* [22] is possible.

Acknowledgments

We thank O. S. Mishina, M. Lewenstein, M. Kubasik, S. R. de Echaniz, and M. Napolitano for helpful discussions. This work was funded by the Spanish Ministry of Science and Education under the LACSMY project (Ref. FIS2004-05830) and the Consolider-Ingenio 2010 Project ‘‘QOIT’’.

Appendix

The atomic ensemble we consider has 10^6 rubidium 87 atoms at a temperature of $30 \mu\text{K}$. For the light we assume a flux $\Phi = 10^{14} \text{ s}^{-1}$ of linearly polarized photons

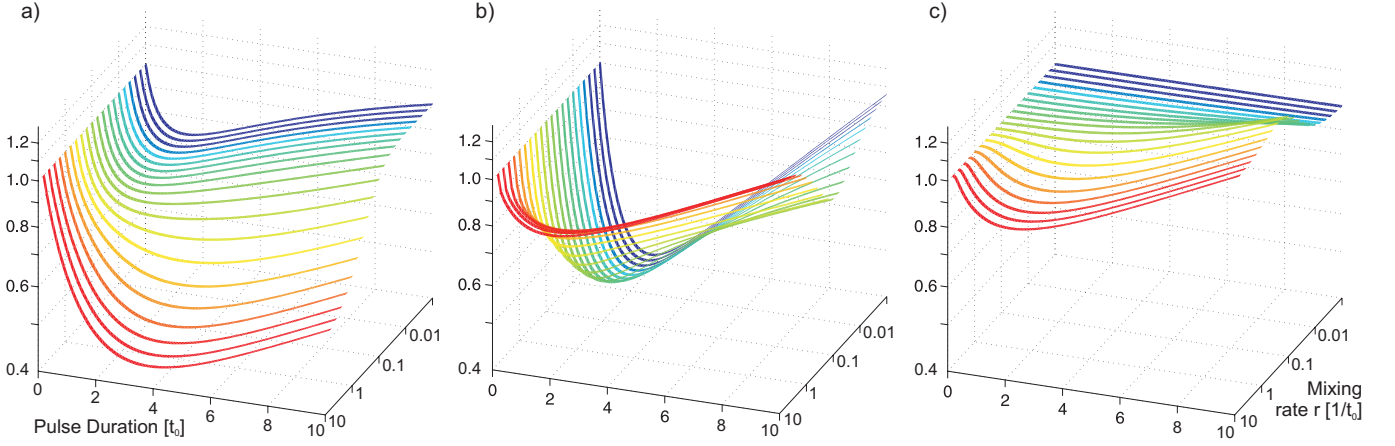


Figure 4: Atomic motion is simulated with different mixing rates. a) shows the degree of spin squeezing for the whole ensemble, b) for the illuminated and c) for the un-illuminated segment. The discussion is given in the text.

with a detuning $\Delta = 1$ GHz from the $F = 1 \rightarrow F' = 0$ transition of the D_2 line. The corresponding wavelength in vacuum is $\lambda = 780.241$ nm. Both atoms and photons interact over a cross section of $A = 4\pi \times 10^{-10} \text{ m}^2$.

The coupling constant g in (26) is directly related to the vector part of the polarizability tensor [21]. For the $F = 1$ hyperfine ground state in the limit of detunings larger than the natural linewidth we find

$$g^{(k,l)} = \frac{1}{A^{(k,l)}} \frac{\Gamma \lambda^2}{16\pi} \frac{1}{\hbar^2} (-4\delta_0(\Delta) - 5\delta_1(\Delta) + 5\delta_2(\Delta)). \quad (35)$$

Where $A^{(k,l)}$ is the interaction cross-section of the segment (k,l) and $\Gamma/2\pi = 6.065$ MHz is the natural line width of the $5P_{3/2}$ excited state. The functions $\delta_{F'}(\Delta) = (\Delta + \Delta_{0,F'})^{-1}$ include the finite hyperfine splittings in the excited state: $\Delta_{0,F'}$ is the hyperfine level spacing between $F' = 0$ and $F' = 1, 2$. It would be straightforward to include inhomogeneity in the local light shift, due to the dipole trap, as $\Delta^{(k,l)}$. However, we don't consider it for the simulations given here.

The scattering probabilities for photons and atoms are given by $\eta_\tau = N_{L,\tau}\sigma(\Delta)/A$ and $\varepsilon = N_A\sigma(\Delta)/A$, as in [14]. Where, A is the interaction area and $N_{L,\tau}$ and N_A the number of photons and atoms in a segment, respectively. The off-resonant atomic scattering cross-section is

$$\sigma(\Delta) = \frac{\lambda^2}{2\pi} \frac{\Gamma^2}{32} \left(4\delta_0(\Delta)^2 + 5\delta_1(\Delta)^2 + 7\delta_2(\Delta)^2 \right), \quad (36)$$

which is valid for detunings much larger than the natural line width.

We derive the characteristic time t_0 . If we apply the interaction (26) for a time τ we find

$$\begin{aligned} \hat{S}'_y &= \hat{S}_y + G\hbar\hat{J}_z\hat{S}_x \\ \hat{J}'_y &= \hat{J}_y + G\hbar\hat{S}_z\hat{J}_x, \end{aligned} \quad (37)$$

where $G = \frac{1}{A} \frac{\Gamma \lambda^2}{16\pi} \frac{1}{\hbar^2} (-4\delta_0(\Delta) - 5\delta_1(\Delta) + 5\delta_2(\Delta))$ similar to (35). The variances are readily calculated for coherent input states (unprimed)

$$\begin{aligned} \text{var}(\hat{S}'_y) &= \frac{\hbar^2}{4} N_{L,t_0} + G^2 \hbar^2 \frac{\hbar^2}{4} N_A \frac{\hbar^2}{4} N_{L,t_0}^2 \\ &= \frac{\hbar^2}{4} N_{L,t_0} \left(1 + G^2 \hbar^2 \frac{\hbar^2}{4} N_A N_{L,t_0} \right) \end{aligned} \quad (38)$$

The same also holds for $\text{var}(\hat{J}'_y)$. When the second term in brackets is unity this describes a signal-to-noise ratio of one and with $N_{L,\tau} = \Phi\tau$ this occurs for $\tau = t_0$ as given in (27). If we use the parameters given above t_0 is $0.55 \mu\text{s}$.

-
- [1] D. J. Wineland, J. J. Bollinger, W. M. Itano, F. L. Moore, and D. J. Heinzen, 1992, Phys. Rev. A **46**, R6797.
 - [2] B. Julsgaard, J. Sherson, J. I. Cirac, J. Fiurasek, and E. S. Polzik, 2004, Nature **432**, 482.
 - [3] L. M. Duan, J. I. Cirac, and P. Zoller, 2002, Phys. Rev.

A **66**, 023818.

- [4] A. Kuzmich, and T. A. B. Kennedy, 2004, Phys. Rev. Lett. **92**, 030407.
- [5] C. P. Sun, S. Yi, and L. You, 2003, Phys. Rev. A **67**, 063815.

- [6] L. B. Madsen, and K. Mølmer, 2004, Phys. Rev. A **70**, 052324.
- [7] P. W. Atkins, and J. C. Dobson, 1971, P. Roy. Soc. Lond. A **321**, 321.
- [8] F. T. Arecchi, H. Thomas, R. Gilmore, and E. Courtens, 1972, Phys. Rev. A **6**, 2211.
- [9] J. M. Radcliffe, 1971, J. Phys. A-Math. Gen. **4**, 313.
- [10] A. Kuzmich, N. P. Bigelow, and L. Mandel, 1998, Europhys. Lett. **42**, 481.
- [11] S. R. de Echaniz, M. W. Mitchell, M. Kubasik, M. Koschorreck, H. Crepaz, J. Eschner, and E. S. Polzik, 2005, J. Opt. Soc. Am. B **7**, S548.
- [12] D. V. Kupriyanov, O. S. Mishina, I. M. Sokolov, B. Julsgaard, and E. S. Polzik, 2005, Phys. Rev. A **71**, 032348.
- [13] B. Demoen, P. Vanheuverzwijn, and A. Verbeure, 1977, Lett. Math. Physics **2**, 161.
- [14] C. Hammerer, K. Mølmer, E. S. Polzik, and J. I. Cirac, 2004, Phys. Rev. A **70**, 044304.
- [15] G. Marsaglia, 1964, J. Amer. Statistical Assoc. **59**, 1203.
- [16] J. Eisert, S. Scheel, and M. Plenio, 2002, Phys. Rev. Lett. **89**, 137903.
- [17] G. Giedke, and J. I. Cirac, 2002, Phys. Rev. A **66**, 032316.
- [18] M. Kitagawa, and M. Ueda, 1993, Phys. Rev. A **47**, 5138.
- [19] J. Sherson, B. Julsgaard, and E. S. Polzik, 2006, *Deterministic atom-light quantum interface* (Elsevier Academic Press), volume 54 of *Adv. At. Mol. Opt. Phy.*
- [20] M. Takeuchi, S. Ichihara, T. Takano, M. Kumakura, T. Yabuzaki, and Y. Takahashi, 2005, Phys. Rev. Lett. **94**, 023003.
- [21] J. M. Geremia, J. K. Stockton, and H. Mabuchi, 2006, Phys. Rev. A **73**, 042112.
- [22] J. Sherson, A. S. Sørensen, J. Fiurasek, K. Mølmer, and E. S. Polzik, 2006, Phys. Rev. A **74**, 011802.
- [23] For atoms in buffer gas vapor cells one can expect a similar behavior.
- [24] Interestingly, one can arrive at the same results for \mathbf{N} and \mathbf{M} assuming a unitary matrix which connects the bosonic atom(light)-modes of different segments. The mixing matrix is then defined as $M_{ij} = |U_{ij}|^2$. Whereas, the noise matrix drops out automatically, when we allow for arbitrary phases between the different input modes and average over them. Which is equivalent to say that atomic mixing is incoherent.